AD-A182 527 FAILURE MODES IN COMPOSITE MATERIALS(U) NAVAL ACADEMY 1/1
ANNAPOLIS MD D A ROBINSON 19 MAY 87 USNA-TSPR-148

UNCLASSIFIED F/G 11/4 NL

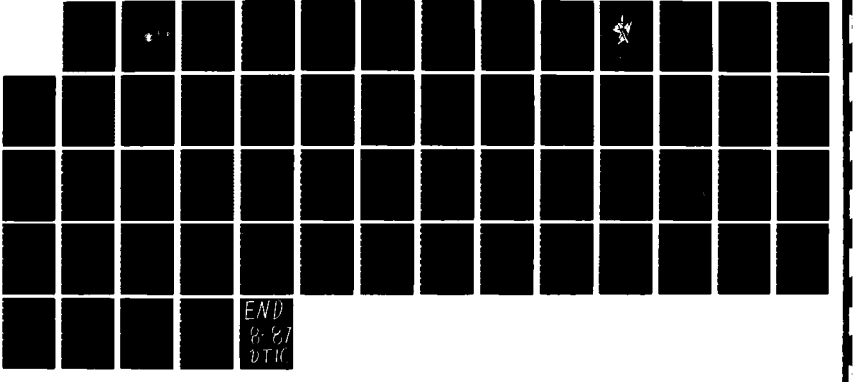

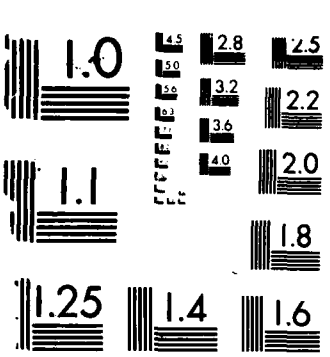

(12)

A TRIDENT SCHOLAR PROJECT REPORT

NO. 148

FAILURE MODES IN COMPOSITE MATERIALS

UNITED STATES NAVAL ACADEMY
ANNAPOLIS, MARYLAND

1987

UNCLASSIFIED

SECURITY CLASSIFICATION OF THIS PAGE (When Date Entered)

REPORT DOCUMENTATION PAGE		READ INSTRUCTIONS BEFORE COMPLETING FORM
1. REPORT NUMBER U.S.N.A. - TSPR; no. 148 (1987)	2. GOVT ACCESSION NO.	3. RECIPIENT'S CATALOG NUMBER
4. TITLE (and Subtitle) FAILURE MODES IN COMPOSITE MATERIALS		5. TYPE OF REPORT & PERIOD COVERED Final 1986/1987 6. PERFORMING ORG. REPORT NUMBER
7. AUTHOR(s) Robinson, David A.		8. CONTRACT OR GRANT NUMBER(s)
9. PERFORMING ORGANIZATION NAME AND ADDRESS United States Naval Academy, Annapolis.		10. PROGRAM ELEMENT, PROJECT, TASK AREA & WORK UNIT NUMBERS
11. CONTROLLING OFFICE NAME AND ADDRESS United States Naval Academy, Annapolis.		12. REPORT DATE 19 May 1987 13. NUMBER OF PAGES
14. MONITORING AGENCY NAME & ADDRESS(if different from Controlling Office)		15. SECURITY CLASS. (of this report) 15a. DECLASSIFICATION/DOWNGRADING SCHEDULE

16. DISTRIBUTION STATEMENT (of this Report)

This document has been approved for public release; its distribution is UNLIMITED.

17. DISTRIBUTION STATEMENT (of the abstract entered in Block 20, if different from Report)

This document has been approved for public release; its distribution is UNLIMITED.

18. SUPPLEMENTARY NOTES

Accepted by the U.S. Trident Scholar Committee.

19. KEY WORDS (Continue on reverse side if necessary and identify by block number)

Composite materials.
Graphite fibers.
Epoxy fibers
Fracture
Fatigue

20. ABSTRACT (Continue on reverse side if necessary and identify by block number)

Presently in all types of materials, mechanical stiffness is an important qualitative and quantitative measure of structural integrity. When a material is repeatedly stressed, some type of internal damage is known to occur which changes the mechanical property of the matter. Although this phenomenon has been long studied in metals, it is not well understood in composites; composites tend to fail instantly with no apparent mechanical warning. If, as is true in the case of graphite and epoxy, the fibers conduct OVER

DD FORM 1 JAN 73 1473 EDITION OF 1 NOV 65 IS OBSOLETE

S N 0102-LF-014-6601

UNCLASSIFIED

SECURITY CLASSIFICATION OF THIS PAGE (When Date Entered)

electricity and the resin does not, then it seems likely that increases in the electrical resistance in the direction of the fibers will indicate the presence of broken fibers and thus be a measure of fatigue damage. Even if resin damage is assumed to play a role in fatigue failure, the breaking of the graphite fibers which do carry the load is an essential step in the reduction of the ultimate strength of the material. This assumption was proven in this experiment. Moreover, it was discovered that the percentage change in electrical resistance was considerably greater than the percentage change in the mechanical stiffness of the material. Consequently, electrical resistance measurements prove to be a sensitive and practical method for detecting internal damage in composite materials which are made up of conducting fibers embedded in a nonconducting matrix.

U.S.N.A. - Trident Scholar project report; no. 148 (1987)

FAILURE MODES IN COMPOSITE MATERIALS

A Trident Scholar Project Report

by

Midshipman First Class David A. Robinson
Class of 1987
United States Naval Academy
Annapolis, Maryland 21412

Associate Prof. O. N. Rask
Advisor - Systems Eng. Dept.

Accepted for Trident Scholar Committee

Chairman

19 May 1987
Date

FAILURE MODES IN COMPOSITE MATERIALS

David A. Robinson

United States Naval Academy

ABSTRACT

Presently, in all types of materials, mechanical stiffness is an important qualitative and quantitative measure of structural integrity. When a material is repeatedly stressed, some type of internal damage is known to occur which changes the mechanical property of the matter. Although this phenomenon has been long studied in metals, it is not well understood in composites; composites tend to fail instantly with no apparent mechanical warning. If, as is true in the case of graphite and epoxy, the fibers conduct electricity and the resin does not, then it seems

likely that increases in the electrical resistance in the direction of the fibers will indicate the presence of broken fibers and thus be a measure of fatigue damage. Even if resin damage is assumed to play a role in fatigue failure, the breaking of the graphite fibers which do carry the load is an essential step in the reduction of the ultimate strength of the material. This assumption was proven in this experiment. Moreover, it was discovered that the percentage change in electrical resistance was considerably greater than the percentage change in the mechanical stiffness of the material. Consequently, electrical resistance measurements prove to be a sensitive and practical method for detecting internal damage in composite materials which are made up of conducting fibers embedded in a nonconducting matrix.

TABLE OF CONTENTS

INTRODUCTION TO FATIGUE IN COMPOSITES

Composite materials are materials consisting of at least two phases. Typically, one phase is fibrous, and the role of the fibers is to provide strength to the material. The second phase is a resin. The resin's role is only to support the fibers, and it adds little strength. With advancements in aerodynamic technology which have enhanced modern aircraft maneuverability to the point where airframes can now withstand more stress than the pilots who fly them, future considerations in the field of aviation include the objectives of increasing range and payload capabilities. Composite materials are a promising step in the achievement of this end, because they can offer the same strength as traditional metals while at the same time being approximately nineteen times lighter.

Today, many combinations of fibers and resins form our advanced fiber reinforced composites. Among the most commonly used fibers are graphite, kevlar, and glass. Presently graphite, or carbon, is the most popular type of fiber, and it is being used extensively in tactical airplanes like the F/A-18 Hornet (see Figure 1) or AV-8B Harrier, and in helicopter rotor blades. Furthermore, carbon composites will account for over half of the structural weight of future tactical airplanes like the Navy and Marine Corp's new V-22 tilt-rotor aircraft, and the

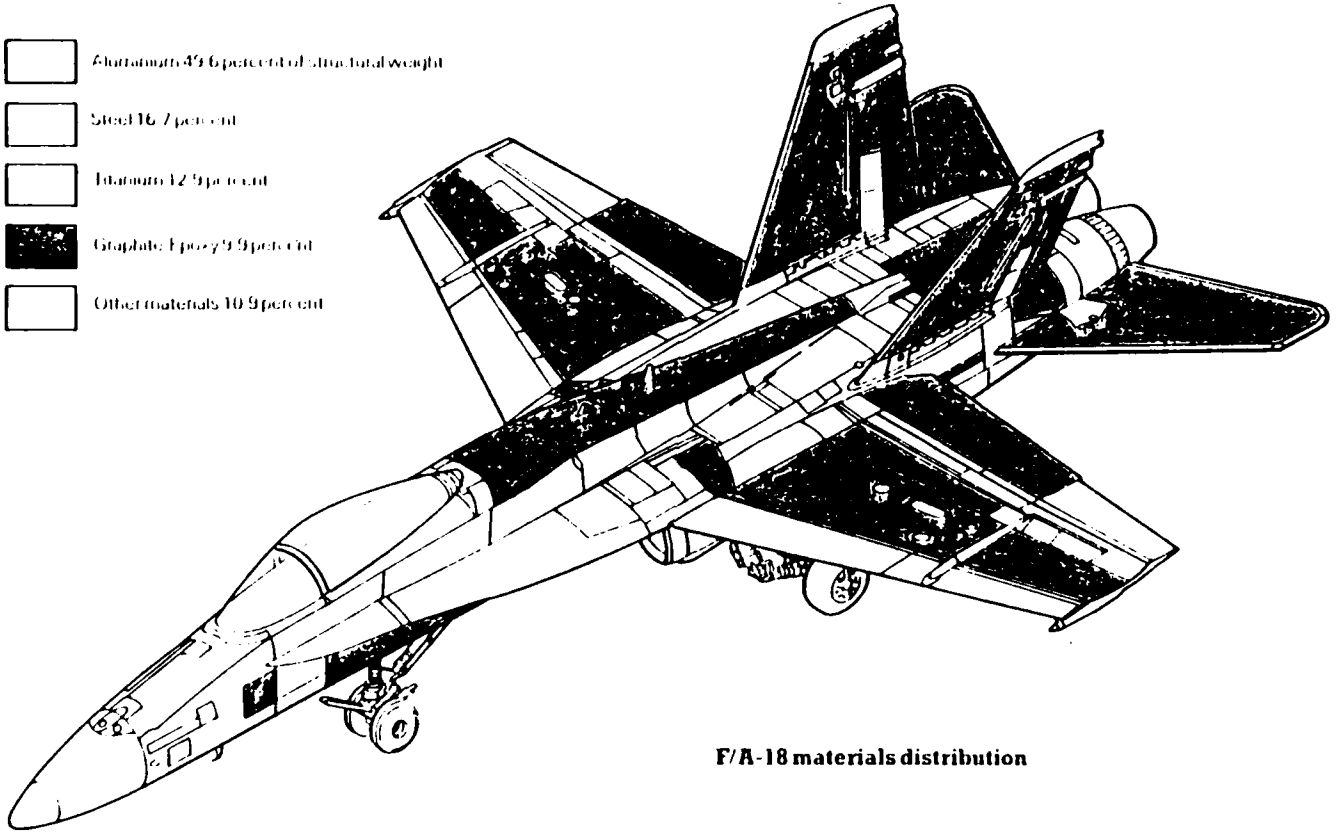

F/A-18 materials distribution

Figure 1

world famous Voyager is made completely out of carbon and epoxy.

Although composites possess the favorable properties of being very strong and yet very light, they also possess a third property which introduces a certain amount of uncertainty with their use. Unlike metals, which tend to show cracks as a structure fatigues, composite structures appear to be perfect right up until the time they break. Consequently, they may fail with no observable warning. As can be imagined, this poses a serious problem when the structure is a propeller or a rotor blade. Since the use of composites in structural applications is relatively new, we have little experience upon which to base any safe estimations concerning a composite's lifespan. In the operational world, this means that we can only guess when a composite part should be retired.

This uncertainty supplies a large portion of the motivation behind this project, with the objective being to study an efficient method of disccvering structural damage before catastrophic failure occurs. The uncertainty can be modelled with the notion that all composite structures contain tiny, unavoidable, built in internal flaws, and that repeated stress will in time accentuate these flaws until they develop to a level at which they can cause failure. However, the randomness in the size and nature of these tiny original flaws, as well as differences in their response to

different types of flexing and fatigue activity causes the uncertainty in the life of composites.

In this project, this problem is viewed through a unique window which has not previously been exploited. Continuous carbon fibers differ from other types of fibers because carbon is an electrical conductor. Additionally, individual carbon fibers can be electrically insulated from each other by the nonconducting matrix in which they are embedded. This allows the properties of fatigue and failure to be approached from an electrical as well as a mechanical point of view.

TEST-SAMPLE CONSTRUCTION

A single carbon filament is about seven millionths of a meter in diameter. Individual fibers can be woven together in various arrangements to form a sheet which is easier to handle. In any structure such as an airframe, composite parts are designed so that these sheets can be bound together in a configuration which will most efficiently contribute to the overall strength and function of the part. To simulate the geometry of a typical aircraft part such as a wing, yet still conform to the physical limits of available testing equipment, careful consideration was given to the test-sample design.

The configuration of the specimen which was ultimately chosen for testing is illustrated in Figure 2. It consists of two layers of unidirectional, G-900 carbon separated by several layers of bidirectional fiberglass, which were all bonded together with epoxy resin. The glass not only served the same purpose that a foam filler would serve in a wing, but it also electrically insulated the two carbon layers.

All of the samples were constructed in the following manner. First, the ends of each of the carbon layers were coated with silver print paint in order to provide a uniform conducting surface. Next, 1/1000 inch thick strips of brass were placed in the paint to act as electrodes. Once the silver paint was dry and the electrodes were securely attached to the fibers, the epoxy was mixed in its correct proportions so that it could be brushed on to a formica surface which allowed for easy removal upon hardening. When the bottom layer of carbon was placed in the epoxy, ensuring that the underside was sufficiently coated, then the resin could be applied to the top side.

At this point, the middle layers of glass were inserted and coated with epoxy. Once the top layer of carbon was placed on top of the glass and brushed with resin, the sample was ready to begin hardening. A synthetic cloth was pressed over the sample to help soak up some of the excess resin, and in 24 hours at room temperature, the hardening process was complete. Finally, the sample could be trimmed

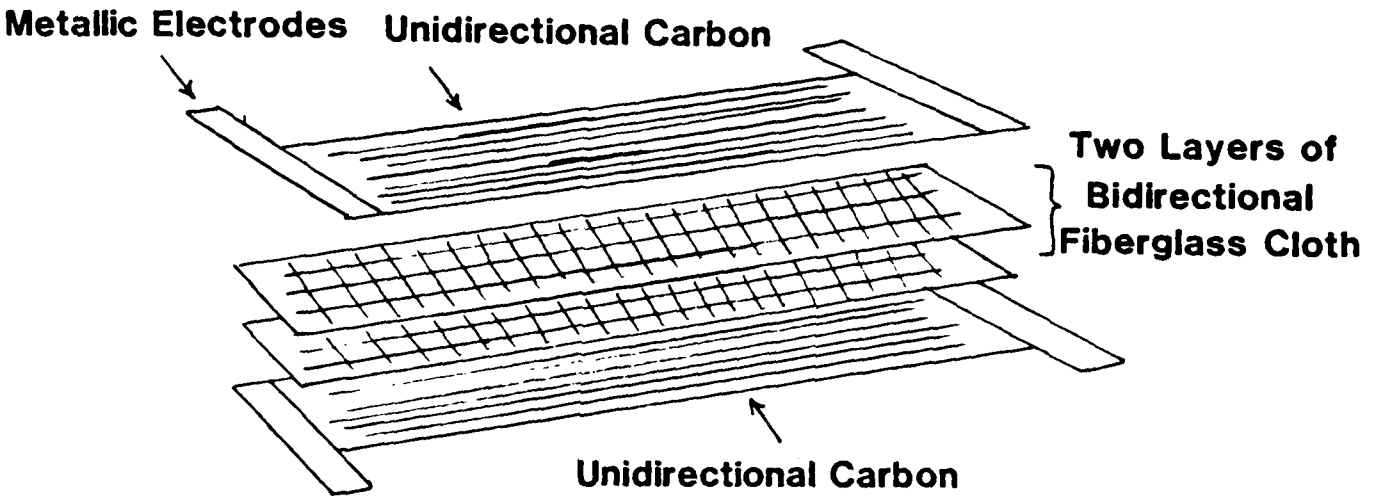

EXPLODED VIEW OF TEST SPECIMEN

Figure 2a

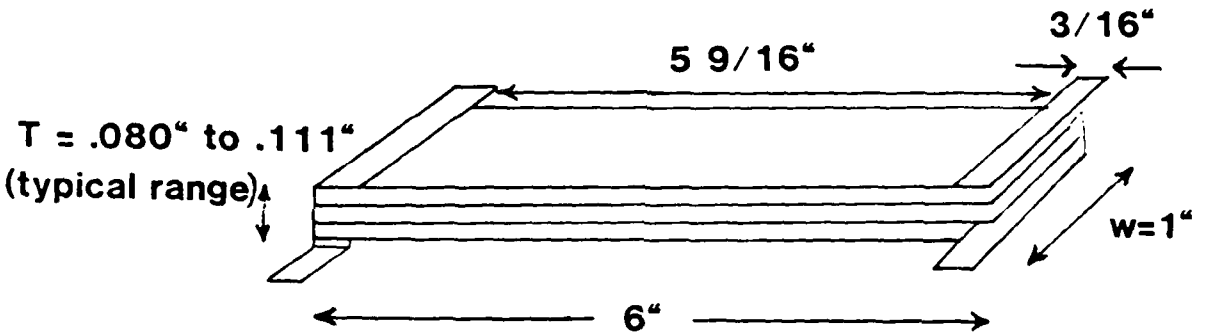

TEST SPECIMEN DIMENSIONS

Figure 2b

to its proper dimensions, and copper wires were then soldered to each of the electrodes to facilitate the use of an impedance bridge in making electrical measurements.

TESTING METHOD

MECHANICAL THEORY

The method which was used for fatiguing and stressing the samples involved a bending process around a given radius of curvature. When a beam, such as a wing, is subjected to bending, the side foremost in the direction of the bend is placed in tension, while the opposite surface is compressed. In a similar way, when one of the samples previously described is bent around a given radius, the top layer of carbon is subjected to tension, while the bottom layer is compressed (see Figure 3). The amount of strain induced in a sample can be accurately known in terms of the ratio of the sample thickness to the radius of curvature (see Appendix F). Furthermore, the length over which this strain affects a sample is directly related to that portion of the sample which actually conforms to the radius when the specimen is displaced in its center. A greater displacement causes an increase in the length of the specimen which conforms to the radius of curvature, and thus the area of a

SAMPLE IN BENDING

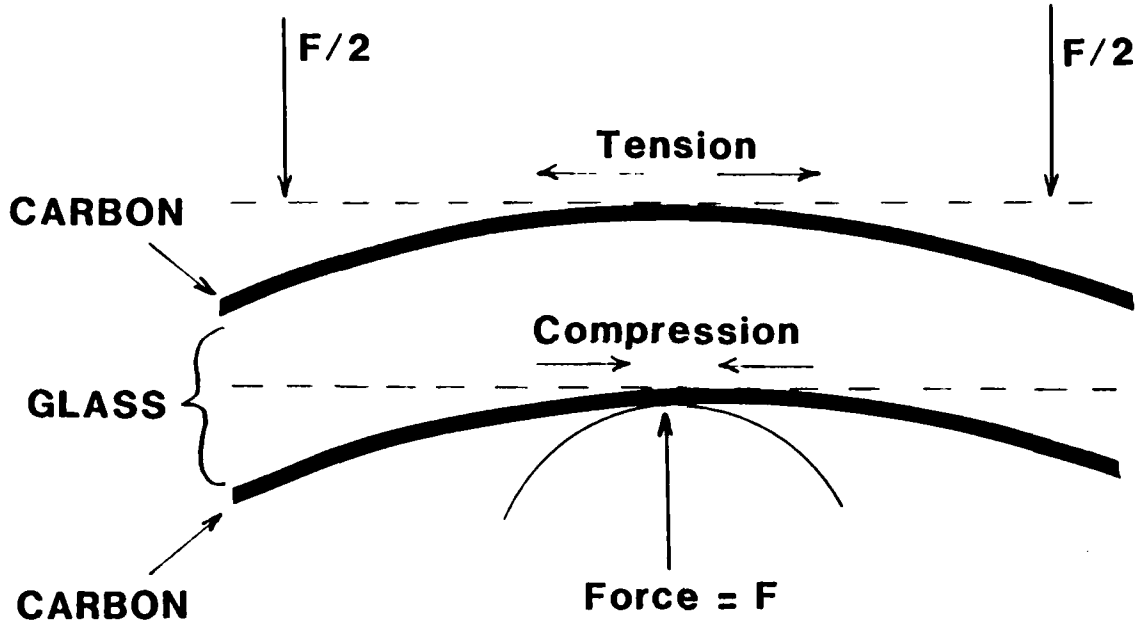

Figure 3

specimen subjected to strain can be varied.

Samples were fatigued hydraulically with a Material Testing System (MTS), which repeatedly flexed the specimen from rest to a given peak strain. The MTS machine was operated in what is termed the stroke control mode as opposed to load control. Under this condition, the mechanical source is what is termed in system theory as an across source. It measures the force, F (lb), required to deliver a known displacement to the center of the specimen. If a known force is applied to the specimen, then it can be said that a through source is being used. The advantage of using an across source in fatigue work is that when a sample begins to fail and its ability to resist a force is reduced, an across source will usually leave the partially damaged specimen intact for additional study whereas a through source will cause the specimen to fail instantly and completely.

The bending configuration which is illustrated in Figure 4 was selected in place of the tension configuration illustrated in Figure 5 for several important reasons. Both tension and compression take place in the bending configuration, and the two stresses occur in different strips of carbon. Consequently, tension and compression fatigue effects can be separated. Furthermore, in the bending configuration of Figure 4, the amount of deflection ranged from .000 inches to .500 inches, and the required

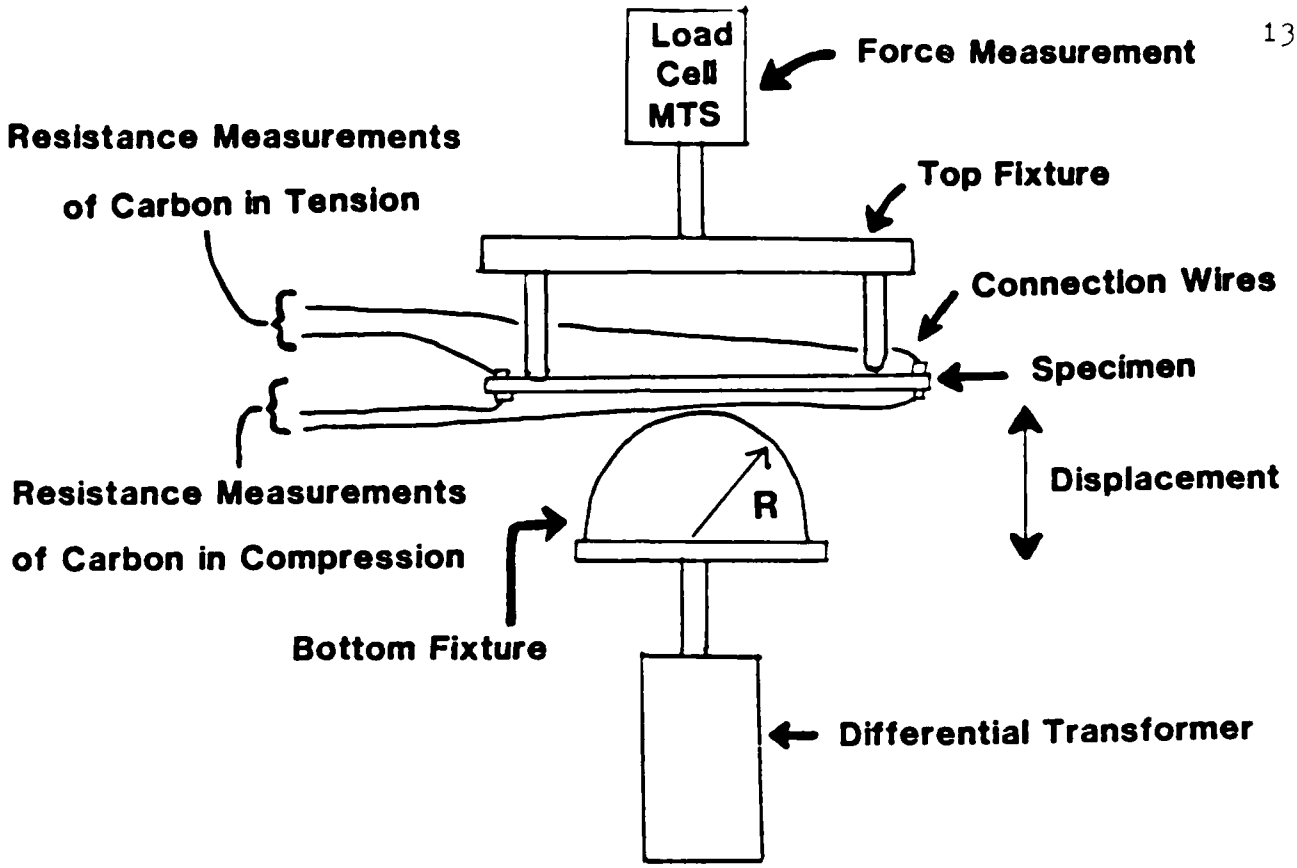

SCHEMATIC DEPICTION OF TEST FIXTURES

Figure 4

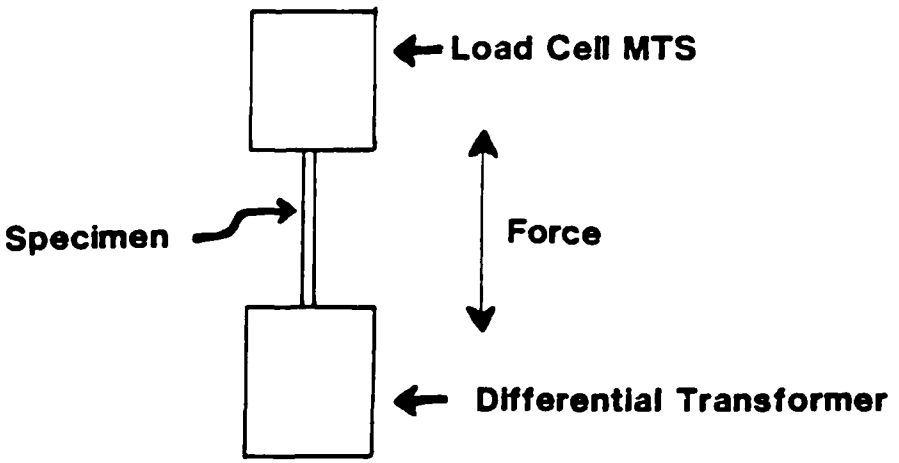

ALTERNATE TEST METHOD

Figure 5

force ranged from 0 to 130 pounds. These magnitudes were conveniently measurable, whereas the process depicted in Figure 5 involved forces up to 2600 pounds which caused the sample to lengthen only .025 inches. Moreover, the bending configuration permitted the sample to be stressed in its center, while at the same time placing no stress on the electrode-fiber interface at the ends. The stability of this electrical connection throughout the life of the specimen is crucial to the accuracy of the experiment, and this stability in the samples was confirmed early in the program.

The testing configuration of Figure 5 has the advantage of simplicity in stress-strain relationships. Hooke's Law, $\sigma = E\delta$ or stress equals the modulus of the material times the strain, can be used in its simplest form to interpret the results. For the bending configuration of Figure 4, the interpretation is slightly more complex.

The interpretation begins with the configuration shown in Figure 6. The deflection, y(x), is a function of the distance, x, from the center of the beam. If it is assumed that dy/dx is small over the entire length, L, then the equation for the deflection, y(x), is given by the expression:

$$EI(d^2y / dx^2) = -(L-x)(F/2) \quad \text{<equation 1>}$$

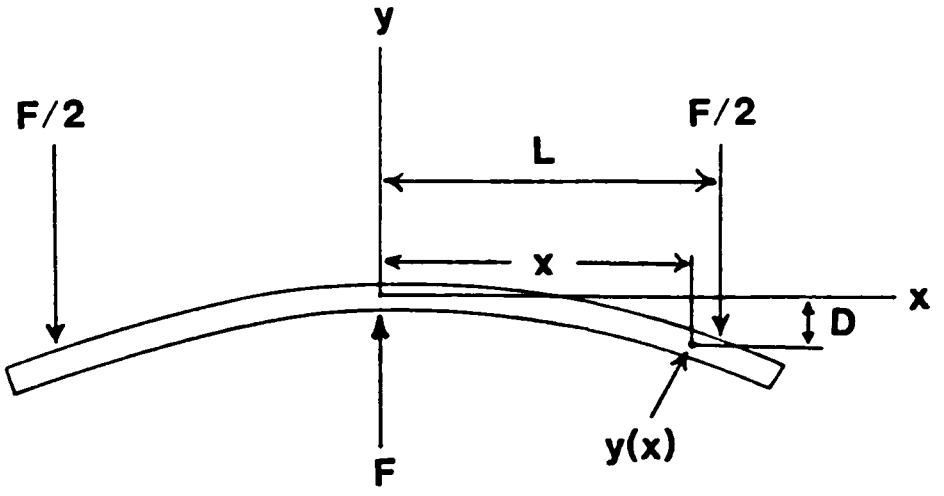

BASIC DEFLECTION

Figure 6

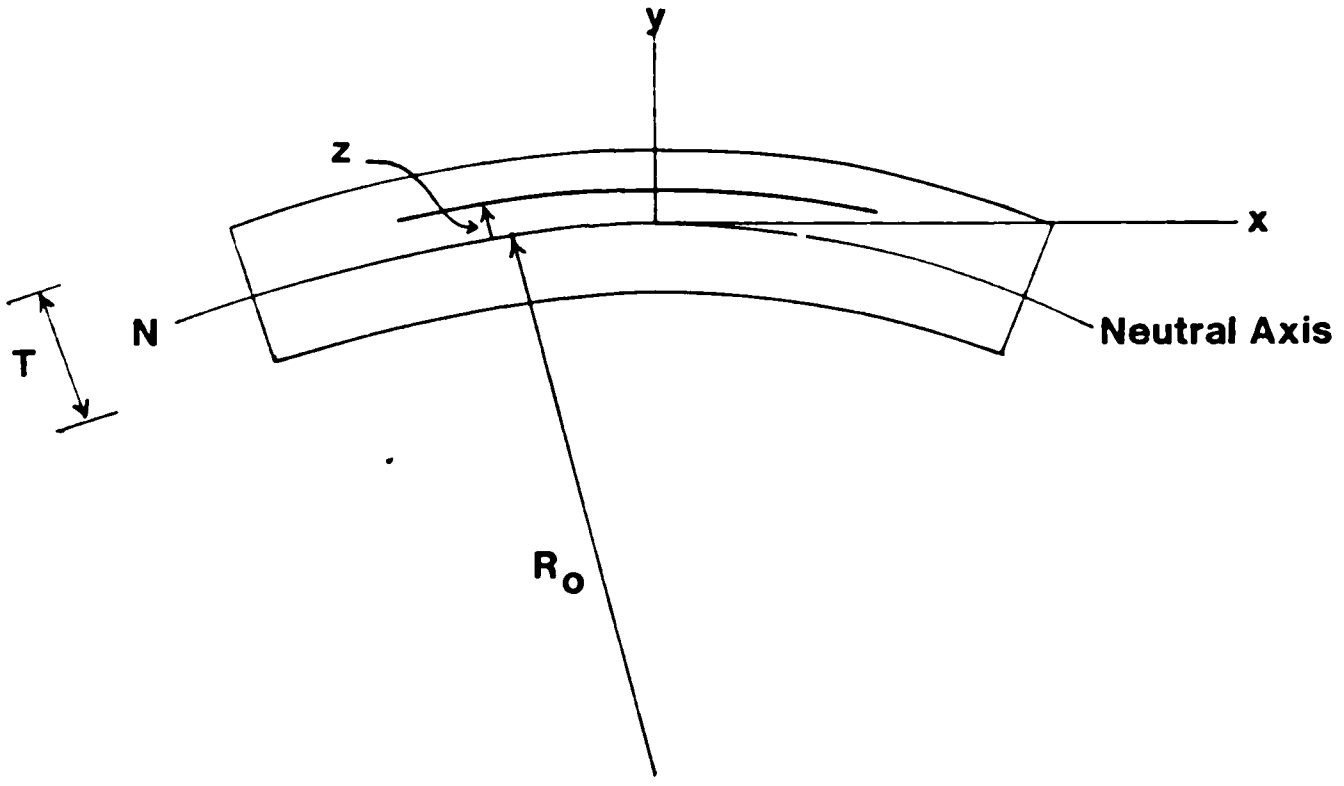

STRAIN AS A FUNCTION OF GEOMETRY

Figure 7

Here E, the modulus of the material, is assumed to be uniform over the beam. I is the moment of inertia of the cross-section of the beam about its neutral axis, and L is half the length of the beam (see Appendix E for actual calculations of EI). This linear, constant coefficient differential equation can be easily solved with the initial conditions $y(0)=0$ and $dy/dx(0)=0$, so that the equation $y(x)$ can be expressed as a function of the force exerted on either end of the beam, F/2. In particular, $y(L)$, which is the maximum deflection that occurs in a sample when the bottom fixture displaces it an equivalent distance, D, can be theoretically related to F/2. The solution is derived in Appendix A, and is:

$$D = -[L^3/3][1/EI](F/2) \quad \text{<equation 2>}$$

The deflection is a linear function of the force, but in this geometry the strain in the material is not simply proportional to the specimen deflection, D. Figure 7 shows a beam bending with a thickness, T, radius of curvature, R_o, and neutral axis, N. If the distance away from the neutral axis to any point within the beam is represented by the letter z, then any strain in the sample can be expressed as $\delta = z / R_o$ (see Appendix B). Since $1/R_o = d^2y/dx^2 = [1/EI](-F/2)(L-x)$, then the strain, δ, can be given approximately as a function of x and z by equation 3:

$$\delta = z/R_o = [z/EI](-F/2)(L-x) \quad \text{<equation 3>}$$

Finally, as is shown in Figure 4, the bottom fixture in the bending configuration is not a point source of force as is suggested in Figure 6, but is a surface with a given curvature, $1/R_o$. Within the scope of this project, three bottom fixtures were used at various times to achieve various results. They had radii, R_o, of .75 inches, 4 inches, and 5 inches with corresponding curvatures of 1/.75 = 1.33 in^{-1}, 1/4 = .25 in^{-1}, and 1/5 = .2 in^{-1}. The advantage of using a bottom fixture with a non-zero radius of curvature is that as the deflection, D, of the testing machine is increased, the resulting maximum curvature of the specimen rises from zero up until it equals the curvature of the bottom fixture. At increasing deflections, the maximum curvature of the specimen will not increase; the region of the specimen in which this maximum curvature is attained increases instead. In this way, a specimen cannot be overstressed by applying too much displacement with the MTS machine.

These simple results only indicate the nature of the considerations actually used to estimate strain in the specimens which were evaluated in this project. However, certain factors were neglected in equations 1, 2, and 3:
1) The curvature is given by $[d^2y/dx^2]/[1+(dy/dx)^2]^{3/2}$ instead of by d^2y/dx^2.

2) The applied force (F/2) is not vertical, but normal to the surface of the specimen at x=L. Friction forces on the surface of the specimen are made approximately equal to zero with the use of teflon tape.

3) The beam is not homogeneous, but consists of carbon surfaces on a fiberglass center. Each carbon strip has a modulus in tension of 12×10^6 lb/in^2 and a modulus in compression of 9×10^6 lb/in^2. The modulus of the fiberglass is estimated to be $1/5(9 \times 10^6)$ lb/in^2. The result is that the neutral axis is not exactly in the center of the beam (see Appendix D).

With these factors included, the shape of the bending beam, y(x), the strain function, $\delta = \delta(x,z)$, and the deflection, D = f(F/2), must be obtained numerically. The use of the Runge-Kutta numerical integration technique in an iterative process allows for the extraction of Figure 8 from all of the considerations mentioned above. The resulting curve represents the displacement of the center of a typical specimen as a function of the applied force, F/2, when the radius of the bottom fixture is assumed to be 5 inches, and EI is assumed to equal 388 lb/in^2. This theoretical graph is considered to be the generic curve associated with the geometry of the bending configuration in Figure 4. The slope of the initial portion of such a curve is taken to be a measure of a sample's stiffness.

THEORETICAL STIFFNESS

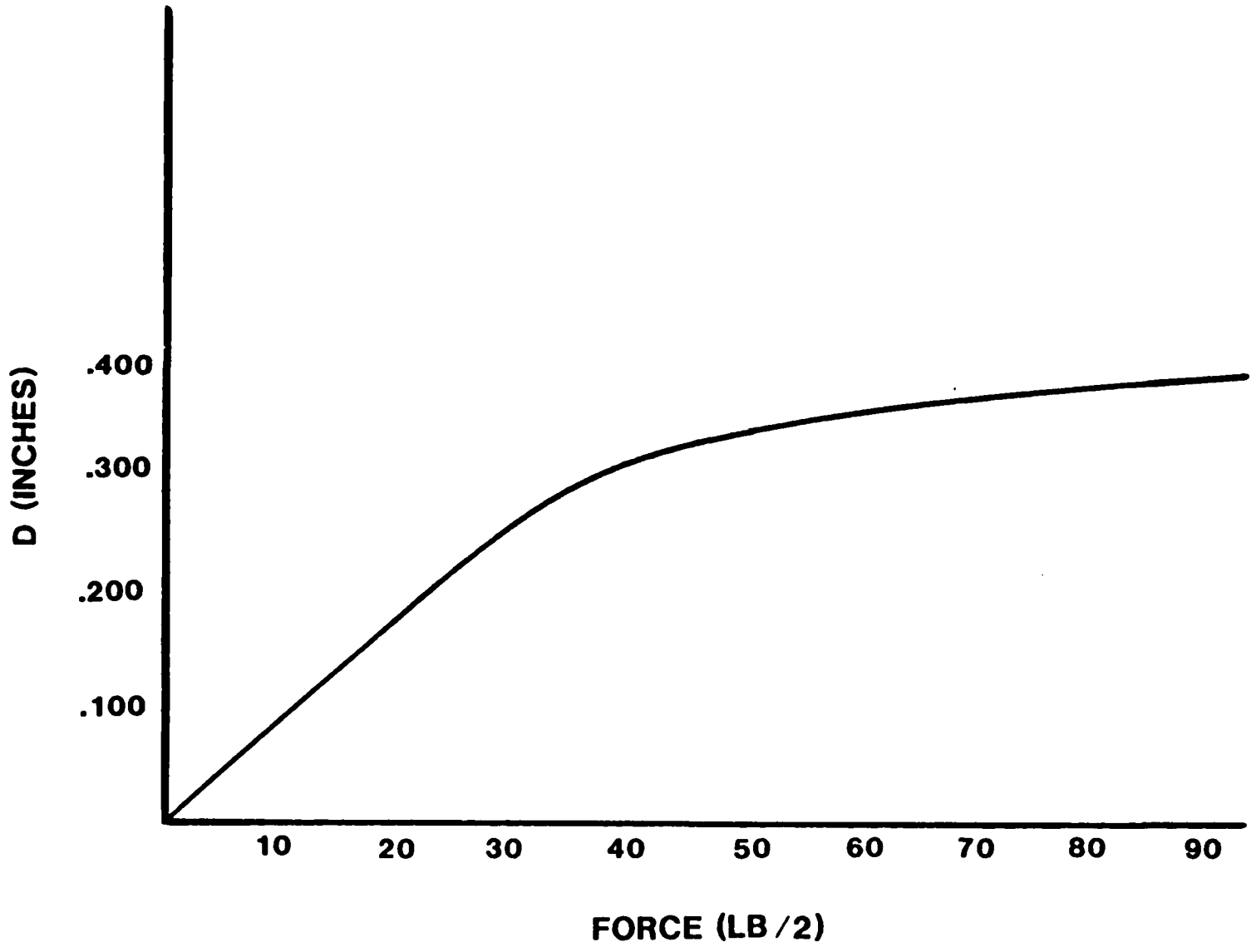

Figure 8

ELECTRICAL THEORY

On a more microscopic level, the forces which act to create tension and compression on the appropriate surfaces of a bending beam or wing also cause the individual fibers in each carbon layer of an experimental sample to stretch if the layer is in tension, and to be compressed if the layer is in compression. Under uniform strain in tension, the electrical resistance of a carbon filament can be expected to rise according to the mathematical expression:

$$R = R_i \left[(1+\delta)/(1 - 2P\delta)\right] \quad \text{<equation 4>}$$

where δ is the longitudinal strain, and P is Poisson's ratio (see Appendix C). Conversely, the resistance will decrease in a similar fashion as a fiber is compressed. When this principle is applied to the approximately 108,000 parallel carbon fibers in each layer, then noticeable resistance changes are detectable as a sample is bent.

In order to obtain the exact expected change in specimen resistance as measured between the electrodes of a sample subjected to the complex strains described earlier, the effects of equation 4 must be numerically summed and evaluated in the manner by which the exact beam deformation was obtained. Once again for a typical specimen with the same parameters that were used to obtain the theoretical

stiffness curve, the theoretical resistance of the upper surface in tension was calculated as a function of the force, F/2. The resulting generic curve is displayed in Figure 9, and it displays the theoretical electrical behavior of a sample's tension surface which is associated with the bending configuration of Figure 4. When the resistance of the compression side is measured, it is found to decrease as expected with increasing force. However, the slope of the resistance curve in compression is less than the slope in tension. This may be attributed to the fact that fibers in compression not only compress, but also tend to buckle.

The typical resistivity of the unstressed carbon itself is given by the manufacturer (Celion) as .089 ohms per square area in the direction of the fibers. Measurements produced in this experiment showed an average of .102 ohms per square area, which shows that the figures correspond closely. No change in resistance per square area in the direction of the fibers occurred when the epoxy was added, and so the electrical resistance, R_i, of a test-sample layer not subject to strain can be estimated to be the distance between the electrodes (5 and 9/16 inches) times the resistance per square area (.102 ohms) which approximately equals 0.6 ohms. When an additional value of 0.1 ohms is added to this figure to account for the constant resistance provided by the electrode connections at both ends of the

THEORETICAL RESISTANCE IN TENSION

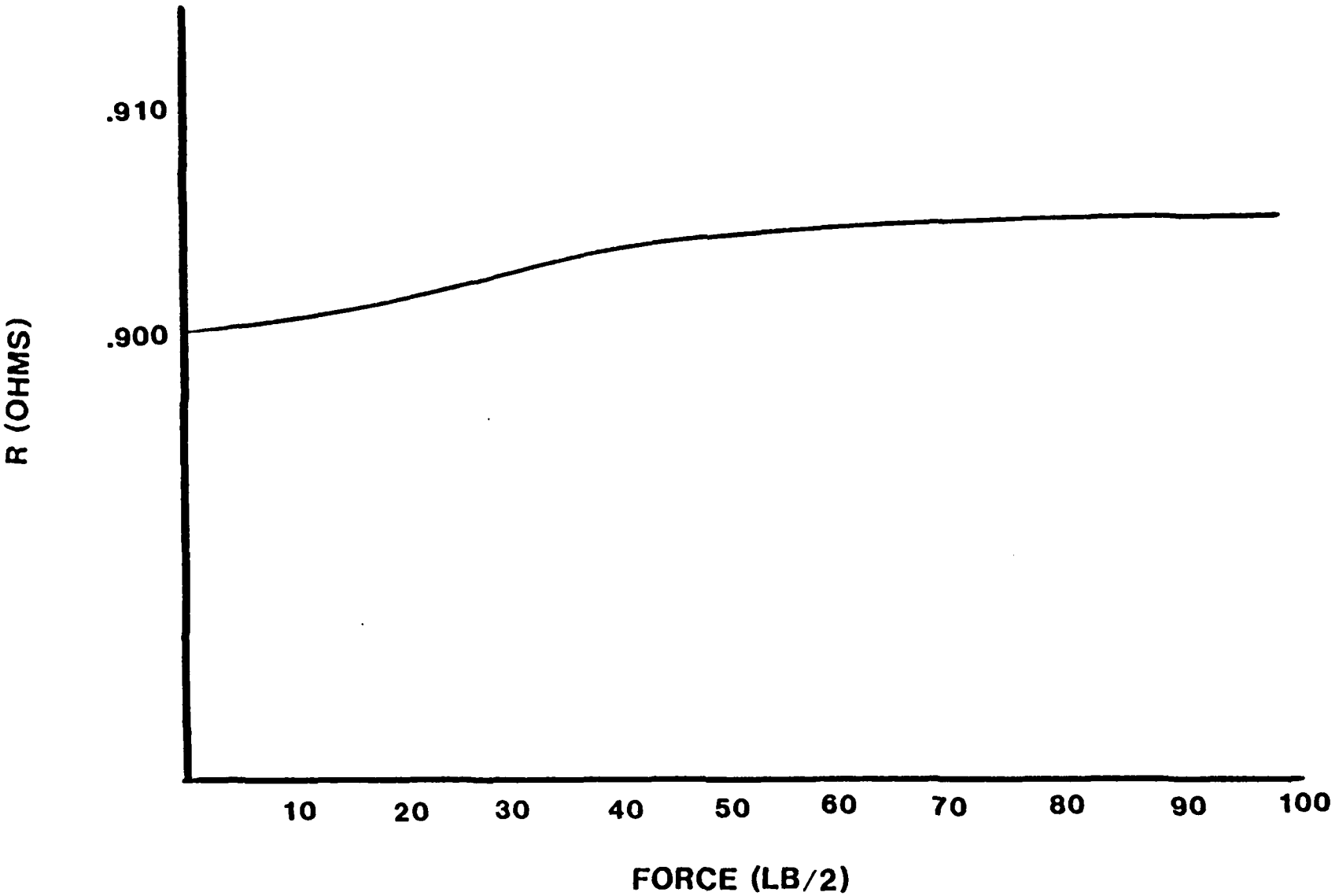

Figure 9

sample, then an overall unstressed resistance of 0.7 ohms is obtained which was the approximate range measured in all of the experimental samples.

The resistance per square area across the fibers of the unidirectional carbon was much more variable, and, as might be expected, it did depend on the presence or absence of the resin. A typical value of resistance per area square across the fibers containing resin is 6800 ohms. The resistance of a unidirectional carbon-epoxy composite is therefore highly directional, with there being almost 5 orders of magnitude difference between the resistances in the different directions.

All resistance measurements were made at 1000 Hz using the 4 point technique which is available on the Wayne Kerr Automatic LCR meter, model #4210. Electrical changes were monitored with an accuracy of four decimal places as samples were flexed from rest to a determined peak strain at a rate of 5 cycles per second for approximately a quarter of a million cycles. Although there was no obvious increase in the temperature of the samples as a result of friction during this process, variations in resistance as a function of temperature were nevertheless considered and the resistance of the samples was found to decrease by .036% per degree Celsius. This figure is far smaller than percentage changes due to force, and thus it was not considered to be significant.

EXPERIMENTAL RESULTS

Because fatigue testing is typically a very lengthy process, the conclusions reached in this project are not supported by large numbers of identical experiments. However, the small number of diverse tests which were performed seem to offer such clear and simple interpretations that it is almost certain that they will be substantiated with repetition. A total of twelve experiments was conducted, which can be divided into separate groups of two and ten. The group of ten tests involved fatigue failure in compression. The remaining two dealt with fatigue failure in tension. These experiments provide three useful insights into the fatigue process.

AFFIRMATION OF THE PRINCIPLE OF UNCERTAINTY

Philosophically, it is easy to believe that any physical object will fatigue with activity. However, if one defines fatigue as repetitive bending at stress levels significantly below a structure's breaking strength, then there are some who say that composites do not fatigue. Several specimens were found to possess a fatigue life which was longer than was practical to measure within the resources available. When the samples were flexed

repetitively to within 70% of their ultimate breaking strength, both the resistance, as measured through the electrode sensors, and the stiffness remained constant until the fatigue process was finally terminated. However, other specimens did fail in a shorter period of time when subjected to the same treatment. This reinforces the original problem of uncertainty in regard to composites by pointing to the fact that their lifespan is unpredictable. But because some samples did fail early, it can be assumed that some flaw was present in the material which the repetitive bending accentuated. Therefore, fatigue can usefully be modeled as the propagation of internal flaws. Those specimens with larger initial flaws failed more rapidly, and within the time interval available for testing. Consequently, initial damage was introduced into the samples in order to start the fatigue process at a higher initial level, thereby causing failure in a shorter period of time.

ELECTRICAL WARNINGS OF INTERNAL DAMAGE

The geometry of the specimens, along with the mechanical properties of the material as given by the manufacturer, can be used to show that the compression surface of the test-specimens should fail before the tension surface. In a particularly useful experiment, damage was

SAMPLE BREAKING IN COMPRESSION

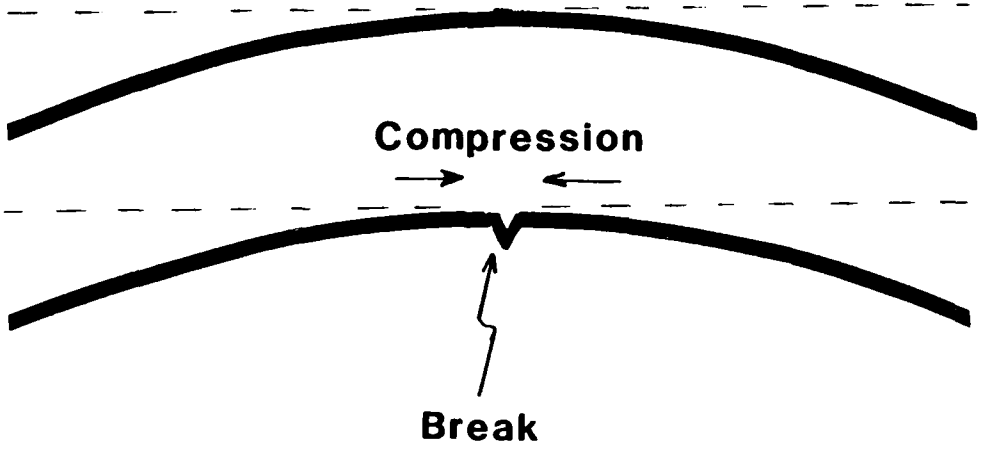

Figure 10

introduced into a sample by overstressing it, which caused a certain fraction of the fibers on the compression side to break (see Figure 10).

During this procedure, the sample was fatigued by the previously mentioned bending process described in Figure 4. Based on the average measured thickness of the specimen, .089 inches, the radius of the bottom fixture, 5 inches, and the mechanical parameters set forth by the manufacturer, the sample could be expected to fail in compression at a displacement, D, of .293 inches.

The nature of the fatigue motion applied was an amplitude oscillation of plus and minus .020 inches about an ever increasing nominal displacement at a frequency of nearly 15 Hz. The intention was to fatigue the specimen at stress levels increasingly closer to the ultimate allowable stress while monitoring the resistance.

At the conclusion of consecutive increments of fatigue exposure consisting of 20,000 cycles each, stiffness and resistance measurements were recorded as a function of force while the sample was flexed from rest to the maximum displacement achieved in the previous exposure. The resulting electrical changes with force are shown by the lower two curves in Figure 11, where the initial no load resistance of the tension surface was nearly .737 ohms, and the initial no load resistance of the compression surface was .788 ohms. As long as no damage occurs, the resistance

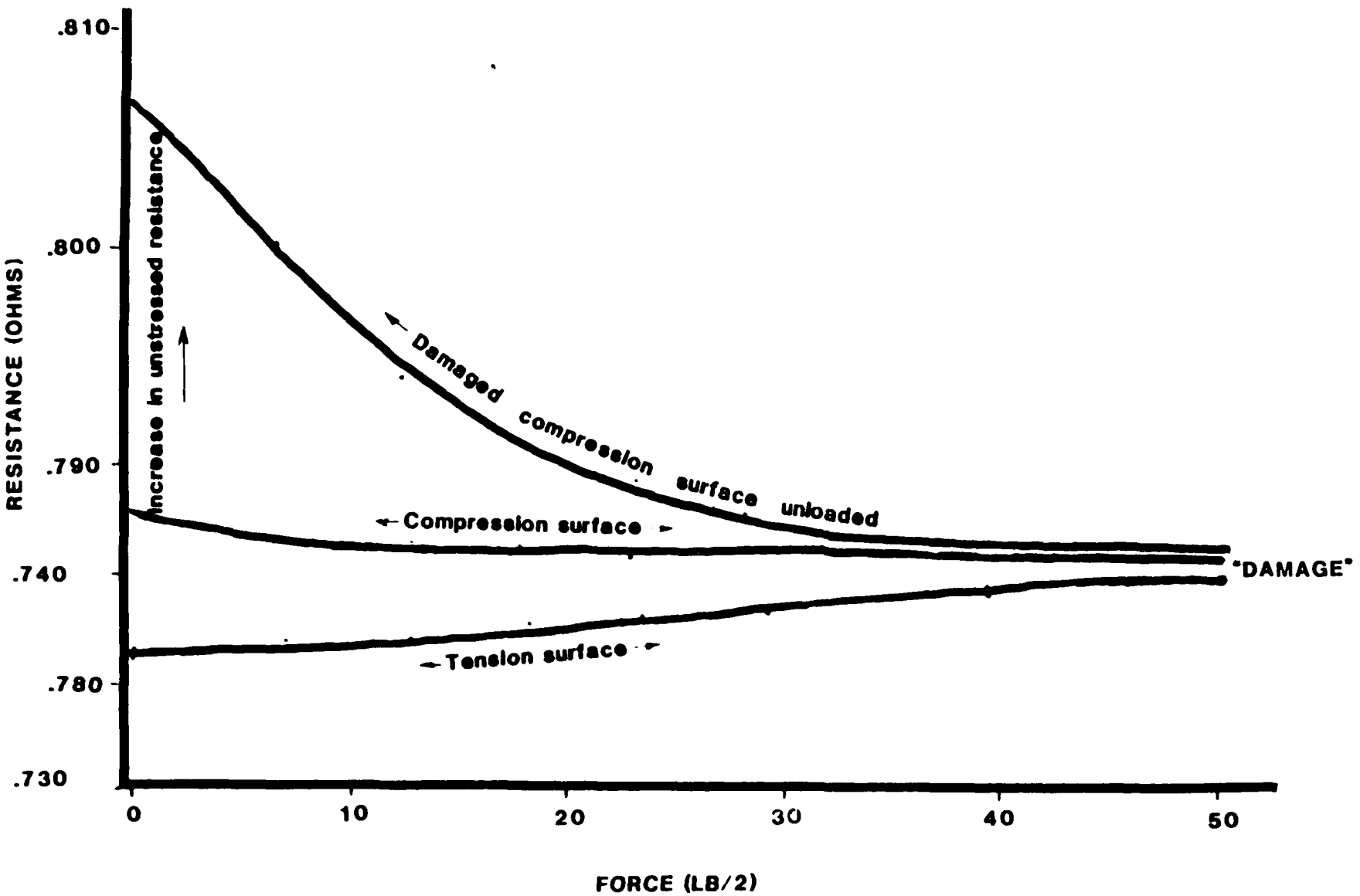
ELECTRICAL CHANGES WITH FORCE
.810
.800
.790
.740
.780
.730
RESISTANCE (OHMS)
Increase in unstressed resistance
Damaged compression surface unloaded
Compression surface
"DAMAGE"
Tension surface
0
10
20
30
40
50
FORCE (LB/2)

Figure 11

curves track up and back along the same line. However in this experiment, when the displacement exceeded .293 inches causing 2.5 inches of the specimen to be stressed 4% over its theoretical limit, some of the fibers in the compression layer were crushed and broken. As the damaged sample was unloaded, these fibers apparently separated (see Figure 12). The resulting open circuits left by these broken fibers caused the unstressed resistance to markedly increase.

At this point, internal damage was present in the sample, and it was clearly noticed electrically. When the stiffness of the specimen was measured at this point, it exhibited no change. A likely interpretation of this is that the broken fibers butt up against each other, and thereby continue to carry their compressive load (see Figure 13). To leap for a moment to the practical implications of this situation, one might suppose that the specimen is a wing spar on an airplane. As long as the damaged side remains in compression, the stiffness of the wing remains the same. But if the airplane were to be inverted, placing the damaged side in tension, then the stiffness could be expected to be slightly less.

To test this hypothesis, the sample was inverted, and the stiffness was found to be reduced by 6.1%. In this case, while the fibers did not butt up against each other, the resin surrounding the few broken fibers can be expected to have carried some of the load (see Figure 14). However,

DAMAGED SAMPLE UNLOADED

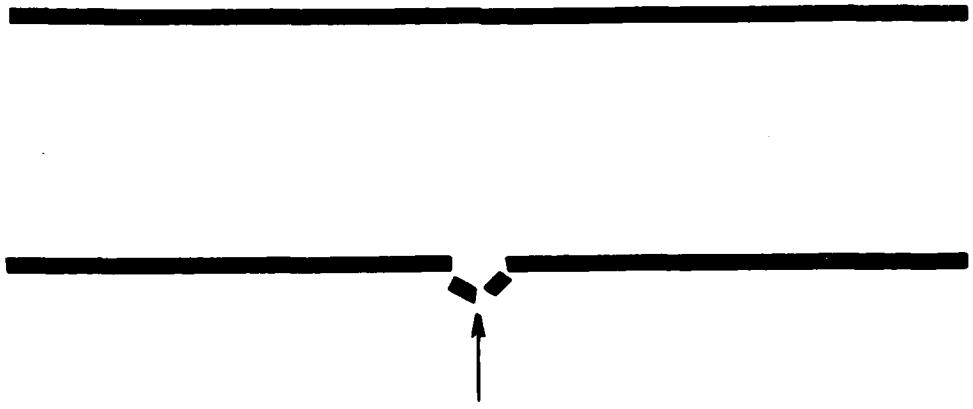

Broken/Separated Fibers

(no electrical contact)

Figure 12

SUPPORT IN COMPRESSION

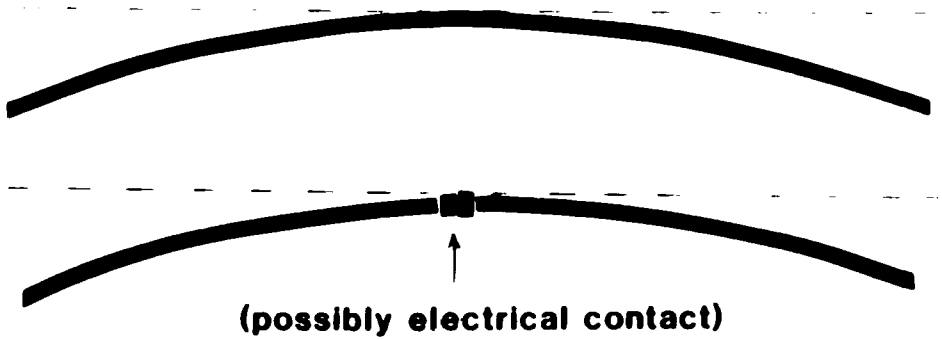

Figure 13

NO SUPPORT IN TENSION

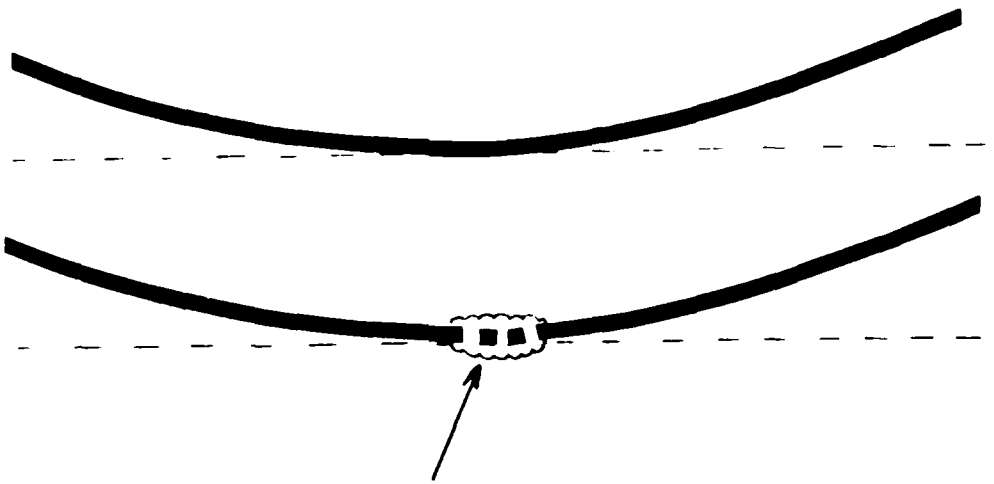

Resin - Small Load Capacity

(no electrical contact)

Figure 14

the resin cannot be expected to contribute to the ultimate strength of the structure since the fibers are the load bearing component of the material.

THE IMPLICATIONS OF RESISTANCE MONITORING

The successful interpretation of the former experiment gives credibility to the approach of using resistance changes to detect internal damage in composite structures. With this approach having been validated, subsequent damage was introduced into the specimens during their construction. An air bubble, which can often exist in the resin of a composite structure, was simulated by placing a drop of silicon grease on the carbon fibers in one of the layers. This prevented the resin from contacting the fibers. Since the function of the resin is to hold the strength providing fibers in position under load, this flaw allowed those fibers in contact with the silicon to flex an extraordinary amount in compression. Further studies showed that such a flaw had little effect in tension, because fibers are stretched through a void in the same way that they are stretched through a matrix. However in compression, this void allowed the compressed fibers to buckle and break, and the resulting abrasion was sufficient to cause rapid deterioration of the sample with fatigue activity.

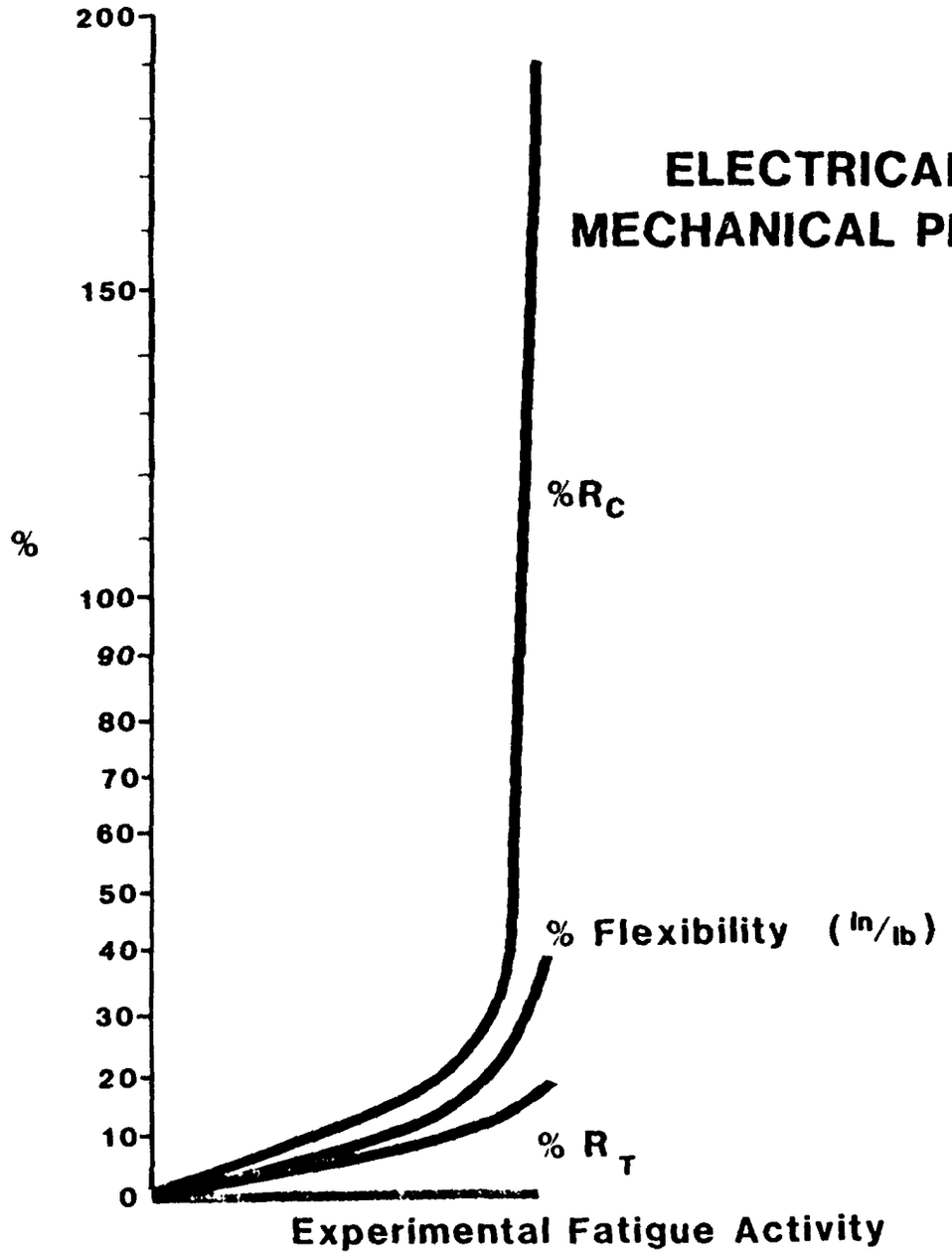
ELECTRICAL VS.
MECHANICAL PROPERTY
200
150
100
90
80
70
60
50
40
30
20
10
0
%
%R_C
% Flexibility ($^{in}/_{lb}$)
% R_T
Experimental Fatigue Activity

Figure 15

The resulting electrical and mechanical properties of the specimen are summarized in Figure 15. Percentage changes in the electrical resistance and mechanical stiffness of the sample are presented as a function of experimental fatigue activity up until the sample failed. The experimental activity consisted of consecutive increments of increasingly severe bending in the same manner as before. The electrical resistance of the undamaged side in tension is represented by the lowest line, R_T. It shows a negligible percentage change, which is expected in a side where no damage has occurred. The two center lines indicate the range of the increase in flexibility of the sample during the fatigue process. The flexibility increases to between 20 and 40 percent, depending on whether the damaged side is placed in tension or compression. Finally, the uppermost line shows the percent increase in the resistance of the layer made vulnerable to damage by fatigue.

The nearly 200% increase in the unloaded resistance, R_C, of the damaged side in compression first suggests that a percentage increase in resistance is a good measure of advancing failure. Presently, continuous stiffness monitoring is an integral part of evaluating damage development. But through a comparison of the resistance curve, R_C, and the two flexibility curves in Figure 15, it is evident that periodic electrical monitoring may perhaps

be a more practical, and is definitely a more sensitive indication of subtle internal damage which can lead to catastrophic failure.

CONCLUSION

In the practical sense, this final discovery implies that an airplane could be pulled into a hangar on a routine basis, a voltage source could be applied across an area where excessive stress is suspected to have occurred, and the resistance could be recorded. If the resistance should increase a substantial percentage since the last recording, then it could mean that it is time to retire the part. Additionally, the possibility exists for monitoring strain internally on an even more frequent basis if resistance measurements are continuously displayed in the cockpit during flight. If dangerous amounts of stress were being exerted on the airframe in a particular maneuver, then this arrangement could warn the pilot of impending failure in time to allow him to return to a less demanding attitude.

FUTURE WORK

As encouraging as these results are, the fact remains

that more measurements are needed to improve the statistics. However, there is a certain degree of confidence associated with these results because they correspond closely to a previous research endeavor in which fatigue failure was shown to occur at about the same reduction in stiffness (Reference 22). A more serious consideration is the need to include metallic electrodes in a load bearing structure. Although this may or may not be ultimately practical in the operational sense, it certainly seems possible in test vehicles where an accelerated aging process could be used to determine an effective maintenance schedule. Additionally, work being done at the Naval Surface Weapons Center in White Oak, Maryland suggests the use of magnetic coupling to induce current in a composite structure in a way that would require no material contact to the fibers. Minor alterations would have to be performed in the specimens used to test this method by placing a few carbon fibers perpendicular to the unidirectional fibers to provide a loop in which the current could flow. In any case, this project was a necessary step toward the objective of using resistance changes to detect internal structural damage in composites. Consequently, the safe application of composites in structural applications looks promising for the future.

REFERENCES

1. Beer, Ferdinand P., Mechanics of Materials, New York: McGraw Hill, 1981.

2. Beetz, C. P., Jr. and Budd, G. W., "Strain Modulation Measurements of Stiffening Effects in Carbon Fibers", Review of Scientific Instruments, Vol. 54(Sept. 83), pp. 1222-26.

3. Clemans, Steve R., Business Development Specialist, Celion Carbon Fibers, Personal Communication, Charlotte, North Carolina, November, 1986.

4. Dally, James W., Experimental Stress Analysis, New York: McGraw Hill, 1978.

5. Ford, Terry, "Rotorcraft Trends: Technologies and Developments", Aircraft Engineering, Vol 57(Nov. 85), pp. 16-18.

6. Gill, R. M., Carbon Fibres in Composite Materials, London: Iliffe Books, 1972.

7. Gray, Reginald I., Research Physicist, Naval Surface Weapons Center, Personal Communication, Dahlgren, Virginia, September, 1986.

8. Gray, Reginald I., Carbon Fiber Electrical Effects-Evaluation Methodology, Dahlgren, Virginia: Naval Surface Weapons Center, 1979.

9. Hansen, Wally, Product Manager, Orcon Corporation, Personal Communication, Annapolis, Maryland, September, 1986.

10. Higden, Archie, Mechanics of Materials, New York: John Wiley and Sons, Inc., 1960.

11. Hull, Derek, An Introduction to Composite Materials, New York: Cambridge University Press, 1981.

12. Jamison, R. D., Mechanical Engineering Department, United States Naval Academy, Personal Communication, Annapolis, Maryland, October-December, 1986.

13. Jones, Robert M., Mechanics of Composite Materials, New York: McGraw Hill, 1975.

14. Lubin, George, Handbook of Composites, New York: Van Nostrand Reinhold Company, 1982.

15. Schwartz, M. M., Composite Materials Handbook, New York: McGraw Hill, 1984.

16. Singer, Ferdinand L., Strength of Materials, New York: Harper and Row, 1962.

17. Sloter, L. E., "Wonder Materials", Wings of Gold, Winter, 1986, pp. 34-36.

18. Tewary, V. K., Mechanics of Fibre Composites, New York: John Wiley and Sons, 1978.

19. Tsai, Stephen W., Introduction to Composite Materials, Lancaster, Pennsylvania: Technomic Publishing Company, Inc., 1980.

20. Vernon, Susan, Research Physicist, Naval Surface Weapons Center, White Oak, Maryland, Personal Communication, Annapolis, Maryland, December, 1986.

21. VanDyne, Peter, Composite Airplane Designer, Builder, and Test-Pilot, Personal Communication, Annapolis, Maryland, January, 1987.

22. Wood, Lawrence E., USNA Trident Scholar project report; no. 140 (1986).

APPENDICES

APPENDIX A

BASIC DIFFERENTIAL EQUATION AND SOLUTION

$$EI(d^2y/dx^2) = (-F/2)(L-x) \quad , \quad y(0)=0 \quad dy/dx(0)=0$$

Taking the Laplace transform of both sides . . .

$$EI[s^2Y(s)-sy(0)-dy/dx(0)] = (-F/2)(L/s - 1/s^2)$$

$$EIs^2Y(s) = (-F/2)(L/s - 1/s^2)$$

$$Y(s) = (-F/2)(1/EI)(L/s^3 - 1/s^4)$$

$$y(x) = (-F/2)(1/EI)(Lx^2/2! - x^3/3!)$$

$$y(L) = (-F/2)(1/EI)(L^3/3) = D$$

APPENDIX B

STRAIN IN A BENT BEAM

(see Figure B)

Strain = δ = Δ length/length

$$\delta = (AA' - BB')/BB'$$

$$\delta = [(R_o + z)\Delta\theta - R_o\Delta\theta]/R_o\Delta\theta$$

$$\delta = z/R_o$$

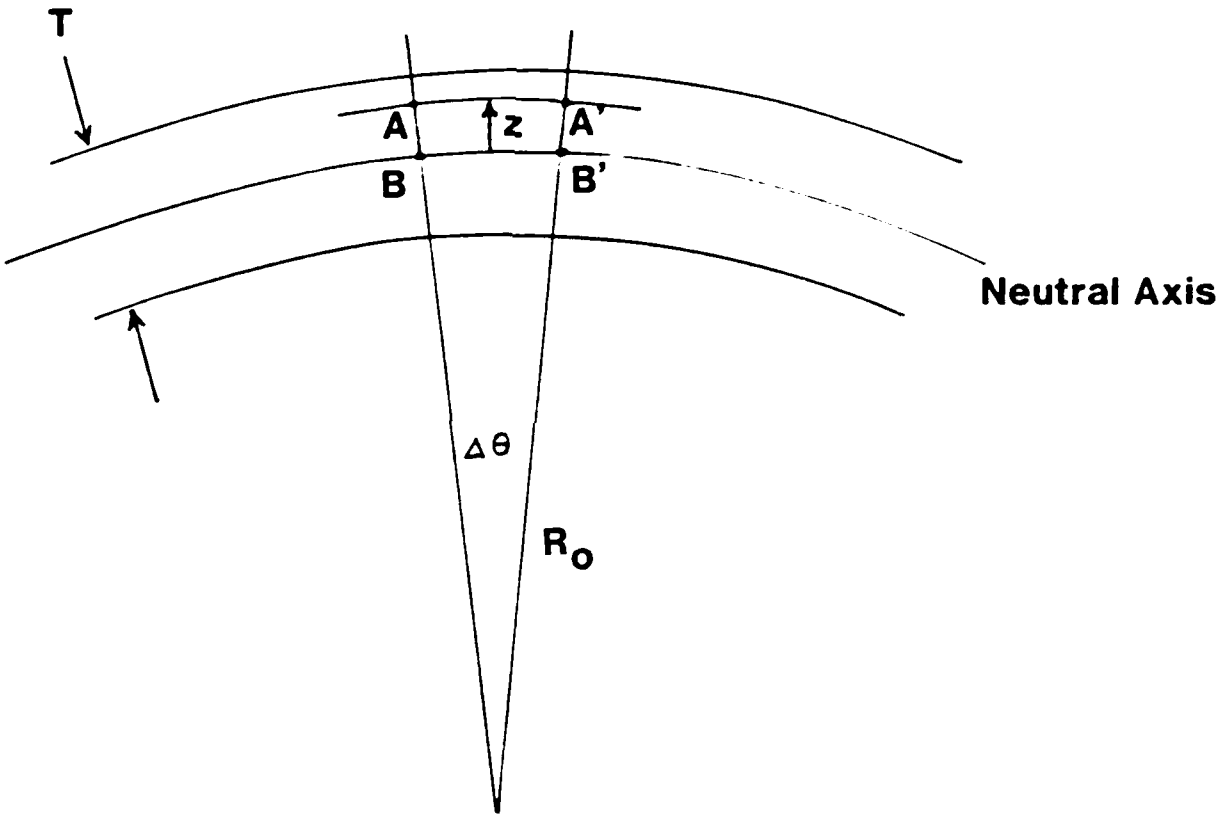

Figure B

APPENDIX C

RESISTANCE CHANGES IN A STRAINED CONDUCTOR

(see Figure C)

$R_i = \rho L_o/A_o$, assuming that ρ is constant during strain. ρ is the electrical resistivity of the material, L_o is the original length, and A_o is the original area. The new length is L, the new area is A, and the change in length is ΔL.

The longitudinal strain, $\delta = \Delta L/L_o$

The transverse strain, $\delta_T = \Delta r/r_o = P(\Delta L/L_o) = P\delta$ where P is Poisson's ratio.

$$\Delta A = (2\pi r_o)\Delta r = (2\pi r_o)(r_o P\delta) = 2\pi r_o^2 P\delta$$

Therefore, $R = \rho[(L_o + \Delta L)/(A_o - \Delta A)]$

$$= \rho[(L_o + \delta L_o)/(A_o - 2\pi(r_o)^2 P\delta)]$$

$$= \rho[(L_o(1+\delta))/(A_o(1-2P\delta))]$$

or, $$R = R_i[(1+\delta)/(1-2P\delta)$$

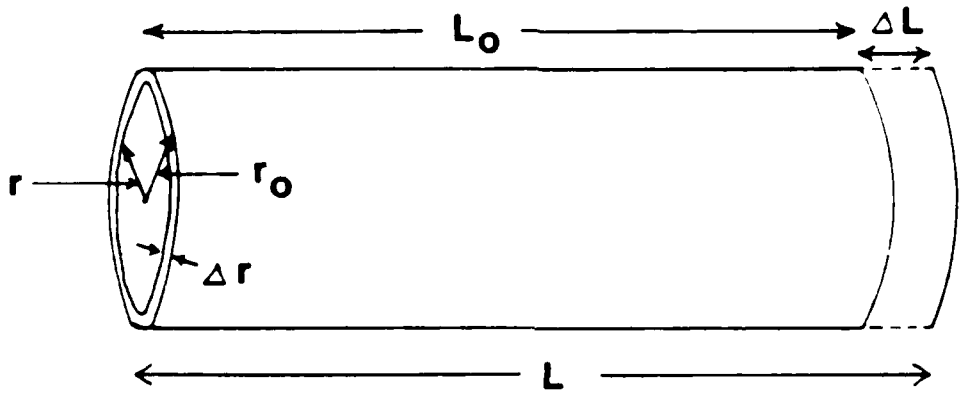

Figure C

APPENDIX D

NEUTRAL AXIS CALCULATIONS

(see Figure D)

The thickness of one layer of G-900 carbon is taken from the manufacturer's published data to be .024 inches. To obtain T_T, which is the distance from the neutral axis to the top of the specimen, the horizontal forces are summed and set equal to zero:

$$\int_{-(T-T_T)}^{-(T-T_T-.024)} E_{CC}(y/R_o)Wdy + \int_{-(T-T_T-.024)}^{0} E_G(y/R_o)Wdy + \int_{0}^{T_T-.024} E_G(y/R_o)Wdy$$

$$+ \int_{T_T-.024}^{T_T} E_{CT}(y/R_o)Wdy = 0$$

where:

E_{CC} is the modulus of carbon in compression = 9×10^6 lb/in^2

E_G is the modulus of glass = $1/5(9 \times 10^6)$ lb/in^2

E_{CT} is the modulus of carbon in tension = 12 x 10^6 lb/in^2

W is the width of the beam (= 1 inch)

R_o is the radius of curvature.

Solution: For T=.080, the above equation when integrated gives:

$$T_T = .036 \text{ inches.}$$

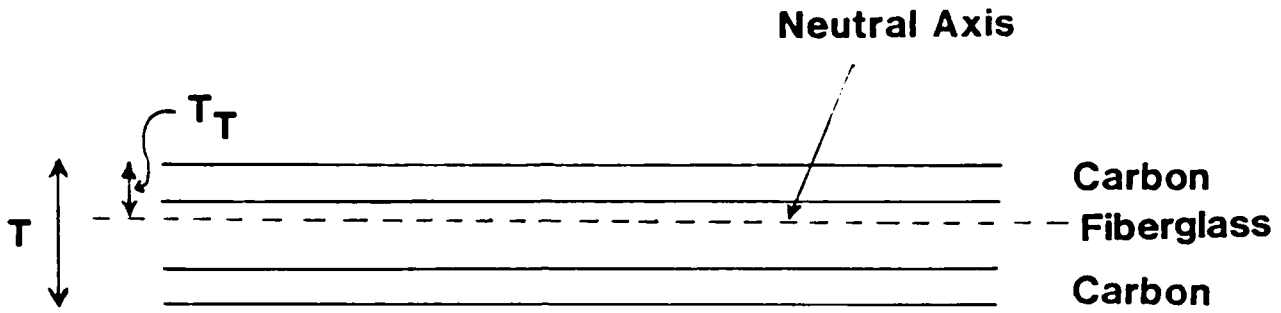

Figure D

APPENDIX E

CALCULATIONS OF EI FOR A COMPOSITE SAMPLE

(see Figure E)

The basic equation for the (half) beam shown in Figure E is derived from the fact that the sum of the moments about point P on the neutral axis at the center of the beam must equal zero. Using the typical dimensions portrayed in Figure E, the equation takes the same form as is found in Appendix D, with the first term being integrated from 0 to .012 inches, the second term from .012 to .036 inches, the third term from 0 to .020 inches, and the fourth term from .020 to .044 inches. For the constants given in Appendix D as well, the moment in the counterclockwise direction is $1/R_o[417]$. The value of 417 lb in ^{2} corresponds to EI in the basic differential equation, and it can be evaluated from the experimental data on displacement as a function of the force, F/2.

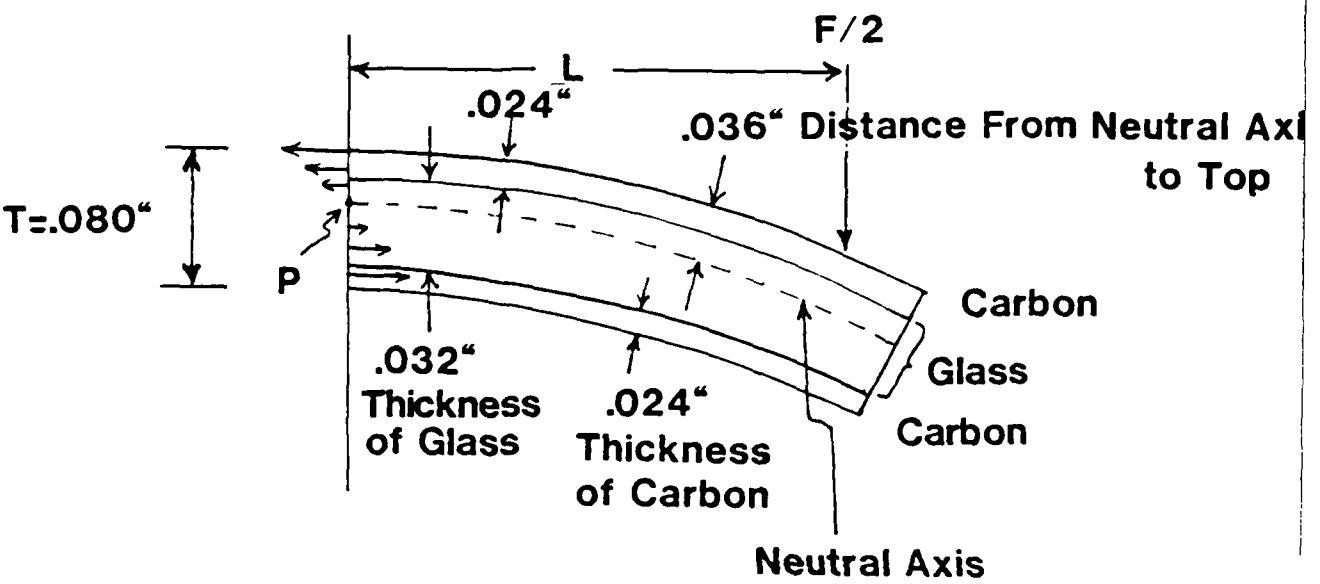
F/2
L
.024"
.036" Distance From Neutral Axi
to Top
T=.080"
P
Carbon
Glass
Carbon
.032"
Thickness
of Glass
.024"
Thickness
of Carbon
Neutral Axis

Figure E

APPENDIX F

STRESS IN CARBON FILAMENTS

(see Figure F)

When a specimen is bent around a curve with a radius of 5 inches, the strain as a function of the distance from the neutral axis is z/5.

The maximum stress in tension is given by:

$$\sigma_{max,T} = E_{CT}(|z|/5) = 12 \times 10^6(z/5) = 12 \times 10^6(.036/5)$$
$$= 8.64 \times 10^3 \text{ psi}$$

The manufacturer gives the maximum allowable stress in tension to be 125,000 psi. Therefore, the top surface is at [86.4/125](100) = 69% of its maximum stress.

The maximum stress in compression is given by:

$$\sigma_{max,C} = E_{CC}(|z|/5) = 9 \times 10^6(.044/5) = 79.2 \times 10^3 \text{ psi}$$

The manufacturer gives the maximum allowable stress in compression to be 90,000 psi. Therefore, the bottom surface is at [79.2/90](100) = 88% of its maximum stress.

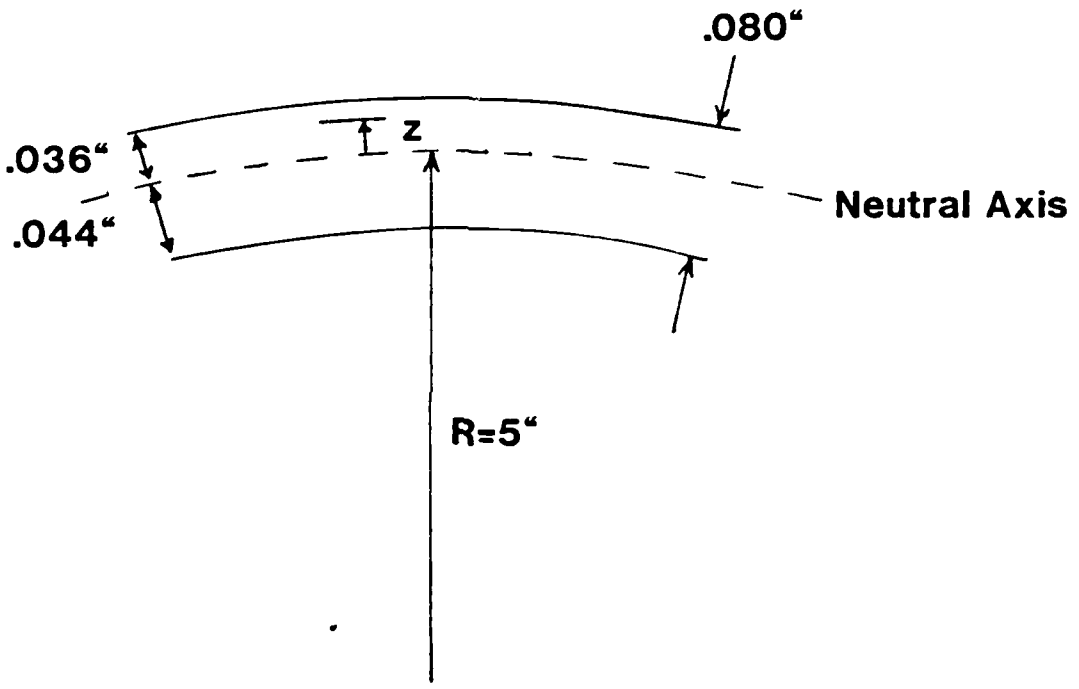

Figure F

ACKNOWLEDGEMENTS

The author wishes to extend his sincerest gratitude to the following people for their special contributions to this project:

- Associate Professor O. N. Rask for his tireless dedication and foresight as the faculty advisor and guiding hand of this research.

- Mr. Reginald I. Gray of the Naval Surface Weapons Center, Dahlgren, Virginia, for his analytic insights.

- Dr. Russell D. Jamison of the Mechanical Engineering Department, United States Naval Academy, for his consulting expertise.

- Mr. Tom Price and the rest of the technicians in the Technical Support Division of the Naval Academy for their skillful solutions and creative methods in overcoming the physical challenges of this project.

- Stanley Womack and the staff of the Materials Lab, DTNSRDC, for the use of their equipment.

END

8-87

DTIC